

Fractal as Julia sets of complex functions via a new generalized viscosity approximation type iterative method

Iqbal Ahmad ^{1,*}, Haider Abbas Rizvi ²

¹*Department of Mechanical Engineering, College of Engineering, Qassim University, Saudi Arabia*

²*Department of Mathematics and Science, College of Arts and Applied Sciences, Dhofar University, Salalah-211, Sultanate of Oman*

Abstract In this article, we study and explore novel variants of Julia set patterns that are linked to the complex exponential function $W(z) = pe^{z^n} + qz + r$, and complex cosine function $T(z) = \cos(z^n) + dz + c$, where $n \geq 2$ and $c, d, p, q, r \in \mathbb{C}$ by employing a generalized viscosity approximation type iterative method introduced by Nandal et al. (Iteration process for fixed point problems and zero of maximal monotone operators, Symmetry, 2019) to visualize these sets. We utilize a generalized viscosity approximation type iterative method to derive an escape criterion for visualizing Julia sets. This is achieved by generalizing the existing algorithms, which led to visualization of beautiful fractals as Julia sets. Additionally, we present graphical illustrations of Julia sets to demonstrate their dependence on the iteration parameters. Our study concludes with an analysis of variations in the images and the influence of parameters on the color and appearance of the fractal patterns. Finally, we observe intriguing behaviors of Julia sets with fixed input parameters and varying values of n via proposed algorithms.

Keywords Algorithms, Escape criteria, Julia sets, Fractals, Iterative methods, Resolvent operator

AMS 2010 subject classifications 70K55, 28A10, 39B12, 47H10

DOI: 10.19139/soic-2310-5070-2089

1. Introduction

There is a significant distinction between Euclidean geometry and non-Euclidean geometry, with the former utilized to model artificial objects while the latter is used to model complicated geometric natural objects. This distinction motivated the invention of distinct modelling techniques. Fractal geometry offers a method for creating complex, aesthetically pleasing objects by applying an iterative process to a simple mathematical function, which is known as a fractal. A fractal is actually an object type where the Hausdorff dimension is larger than its topological dimension, and its boundary or surface is extremely rough [12]. The Julia sets of the complex polynomial $z^p + c$, where $c \in \mathbb{C}$ is a parameter, were produced by Lakhtakia et al. [12]. In [2], both rational complex functions and the transcendental were studied. Fractals are being applied for various purposes these days, such as in cryptography, image encryption or compression, art and design, and pattern recognition (see, [13, 16, 19, 20, 21, 22, 29, 30]). The applications of fractal theory revolutionized the industries of security control systems, radio, capacitors, radar systems, and antennas for wireless systems (see [3, 10, 13, 18]).

Numerous methods have been used to investigate and visualise fractals (see [1, 7, 9, 19, 20]). The escape criterion plays a prominent role in the generation of fractals (particularly, Julia and Mandelbrot sets), which is a stopping criterion based on the number of iterations needed to determine whether the orbit of an initial point escapes to

*Correspondence to: Iqbal Ahmad (Email: i.ahmad@qu.edu.sa). Department of Mechanical Engineering, College of Engineering, Qassim University, Saudi Arabia.

infinity or not. Through a various iterative procedures, it has been established that this criterion is a suitable mechanism to illustrate the characteristics of dynamical systems.

Mann [15] proposed the Mann iterative method, an averaged iterative technique. However, in general, this method does not converge strongly. Numerous modified forms of the Mann iteration technique have been investigated to achieve strong convergence. In 1967, Halpern [4] introduced one of the most significant iterative methods for finding a fixed point of nonexpansive type mappings. In 2000, Moudafi [14] introduced the viscosity approximation method which is a well known generalization of the Halpern method that is frequently used to approximate a fixed point of a nonexpansive mapping and other kinds of non-linear mappings (see [17, 25, 26, 29] and the references therein).

In the literature, Mann and similar types of fixed point iterative methods have been used so far for generating these fractals. For example, the explicit types of iterations are: Mann iteration [22, 23], Picard-Mann iteration [30], Picard-Mann iteration with s -convexity [24], Ishikawa iteration [21], S-iteration [8], SP iteration [20], RK iteration [5], and the implicit ones: Jungck-S iteration [11], Jungck-CR iteration [27] etc. Nandal et al. [17] introduced and studied a generalized version of the viscosity approximation type iterative methods in Hilbert space. They applied their method to solve various problems, such as the general system of variational inequalities, convex feasibility problems, zero point problems of inverse strongly monotone and maximal monotone mappings, split common null point problems, split feasibility problems, split monotone variational inclusion problems, and split variational inequality problems. We discovered that the suggested iterative procedure has several applications in the field of fixed point theory and that it also has the potential to generate fractals (see [25, 26]).

Motivated by this fact, our paper used this new type of generalized viscosity approximation type iterative method for generating fractals as Julia sets. The rest of the paper is organized as follows: Sect. 2 deals with the basic definitions and facts. In Sect. 3, we derive the escape criterion that is used to draw Julia sets for complex exponential functions, i.e., $W(z) = pe^{z^n} + qz + r$, and complex cosine functions i.e., $T(z) = \cos(z^n) + dz + c$, where $n \geq 2$ and $c, d, p, q, r \in \mathbb{C}$. Next, in Sect. 4, we present pseudo-codes of escape time algorithms for generating Julia sets via the proposed iteration method. Moreover, we present some graphical examples of the sets obtained with those algorithms. Finally, we conclude our work in Sect. 5.

2. Preliminaries

In this section, we give some basic definitions and facts from the literature for the completeness of the paper.

Definition 2.1 (Julia set [6])

Let $W : \mathbb{C} \rightarrow \mathbb{C}$. The filled Julia set of W is denote by \mathcal{Q}_W and is defined as

$$\mathcal{Q}_W = \{z \in \mathbb{C} : \{|W^k(z)|\}_{k=0}^{\infty} \text{ is bounded}\}.$$

where W^k denotes the k^{th} iteration of the function W . Noticeably, it is a set of complex numbers for which the orbits do not converge to a point at infinity. The Julia set of W is the boundary of \mathcal{Q}_W , that is, $\mathcal{Q}_W = \partial\mathcal{Q}_W$.

In 2000, Moudafi [14] investigated the viscosity approximation method. In the complex plane, this method can be defined as

Definition 2.2 ([14])

Let $W : \mathbb{C} \rightarrow \mathbb{C}$ be a complex mapping. For an initial point $z_0 \in \mathbb{C}$, consider the following sequence $\{z_k\}$ of iterates

$$z_{k+1} = \beta_k g(z_k) + (1 - \beta_k)W(z_k), \quad k \geq 0, \quad (2.1)$$

where $\beta_k \in (0, 1)$ and $g : \mathbb{C} \rightarrow \mathbb{C}$ is a contraction mapping. The iterative method given in (2.1) is called the *viscosity approximation method*.

Remark 2.1

The viscosity approximation iterative method reduces to the Halpern iteration [4] if we consider the mapping g as a constant mapping, i.e., $g(z) = b$, where $b \in \mathbb{C}$.

In 2021, Nandal et al. [17] considered a new generalized viscosity approximation-type iterative method. In the complex plane, this method can be defined as follows: starting with an arbitrary initial point $z_0 \in \mathbb{C}$, the sequence $\{z_k\}$ generated by

$$\begin{cases} z_{k+1} = \mathcal{J}_\lambda^{B_1} T_j^k T_{j-1}^k \cdots T_2^k T_1^k y_k, \\ y_k = \alpha_k g(z_n) + (1 - \alpha_k) \mathcal{J}_\mu^{B_2} U_k z_k, \end{cases} \quad (2.2)$$

where g is a contraction mapping, $U_k = (1 - \beta_k)I + \beta_k U$, and $T_l^k = (1 - \gamma_k^l)I + \gamma_k^l T_l$, for $l = 1, 2, \dots, j$, with $\alpha_k, \beta_k, \gamma_k^l \in (0, 1)$, the resolvent operators $\mathcal{J}_\lambda^{B_1} = (I + \rho_k B_1)^{-1}$ and $\mathcal{J}_\mu^{B_2} = (I + \mu_k B_2)^{-1}$ are associated with monotone operators B_1 and B_2 , respectively, with $\lambda_k, \mu_k \in (0, \infty)$.

Let us consider the following complex mapping $W, T : \mathbb{C} \rightarrow \mathbb{C}$ as:

$$\begin{cases} W(z) = pe^{z^n} + qz + r, \\ T(z) = \cos(z^n) + dz + c, \end{cases} \quad (2.3)$$

where $n \geq 2, p, q, r, d, c \in \mathbb{C}$ and let g be a complex contraction mapping on \mathbb{C} , i.e., $g(z) = az + b$ with $a, b \in \mathbb{C}$ and $|a| < 1$.

To generate fractals and escape limitations are the basic key to run the algorithms. Since it is well known that $|\cos(z^n)| \leq 1$ for some $z \in \mathbb{C}$ and the Maclaurin expansion for sine and exponential functions are

$$|\cos(z^n)| = \left| \sum_{k=0}^{\infty} \frac{(-1)^k z^{2nk}}{(2k)!} \right| > |z^n| \left| \sum_{k=1}^{\infty} \frac{(-1)^k z^{n(2k-1)}}{(2k)!} \right| \geq |\omega_1| |z^n|, \quad (2.4)$$

where $0 < |\omega_1| \leq 1$ except the values of $z \in \mathbb{C}$ for which $|\omega_1| = 0$ and satisfying the bound

$$\left| \sum_{k=1}^{\infty} \frac{(-1)^k z^{n(2k-1)}}{(2k)!} \right| \geq |\omega_1|$$

and

$$|e^{z^n}| = \left| \sum_{k=0}^{\infty} \frac{z^{nk}}{k!} \right| > \left| \sum_{k=1}^{\infty} \frac{z^{nk}}{k!} \right| = |z^n| \left| \sum_{k=1}^{\infty} \frac{z^{n(k-1)}}{k!} \right| > |\alpha| |z^n| \quad (2.5)$$

where $0 < |\alpha| \leq 1$ and satisfying the bound $\left| \sum_{k=1}^{\infty} \frac{z^{n(k-1)}}{k!} \right| > |\alpha|$, (see, [10, 28]).

3. Escape criteria for the considered complex functions

Let us assume that $j = 2$, and that we use constant sequences $\alpha_k = \alpha, \beta_k = \beta, \gamma_k^1 = \gamma, \gamma_k^2 = \delta, \lambda_k = \lambda, \mu_k = \mu, T_1^k = V, T_2^k = S$, where $\alpha, \beta, \gamma, \lambda \in (0, 1)$ and $\lambda, \mu \in (0, \infty)$. Let us assume that $g(z) = az + b$ is a complex contraction mapping with $a, b \in \mathbb{C}$ and $|a| < 1$, and that $B_1(z) = \omega z$ and $B_2(z) = mz$, where $\omega, m \in \mathbb{R}$. Thus, $\mathcal{J}_\lambda^{B_1}(z) = \frac{z}{1+\omega\lambda}$ and $\mathcal{J}_\mu^{B_2}(z) = \frac{z}{1+m\mu}$. Also, let $U = V = W$ and $S = g$, where W is given in (2.3). For such parameters the iteration (2.2) takes the following form:

$$\begin{cases} z_{k+1} = \mathcal{J}_\lambda^{B_1} S_\delta V_\gamma y_k, \\ y_k = \alpha g(z_n) + (1 - \alpha) \mathcal{J}_\mu^{B_2} U_\beta z_k, \end{cases} \quad (3.1)$$

where $U_\beta = (1 - \beta)I + \beta U, V_\gamma = (1 - \gamma)I + \gamma V$, and $S_\delta = (1 - \delta)I + \delta S$.

3.1. Escape criterion for $W(z) = pe^{z^n} + qz + r$

In this section, we prove the escape criteria for transcendental function $W(z) = pe^{z^n} + qz + r$, where $n \geq 2, p, q, r \in \mathbb{C}$ via generalized viscosity approximation-type iterative method.

Theorem 3.1

Let $W(z) = pe^{z^n} + qz^2 + r$ be a complex function, where $n \geq 2, p, q, r \in \mathbb{C}$. Assume that $z_0 \in \mathbb{C}, |z_0| \geq \max\{|r|, |b|\} > \max\left\{\left(\frac{(1+\alpha(1+|a|))|1+m\mu|+(1-\alpha)(1+\beta|q|)}{(1-\alpha)\beta|p||\omega_1|}\right)^{\frac{1}{n-1}}, \left(\frac{(1+\gamma|q|)}{\gamma|p||\omega_2|} + \frac{(\delta+|1+\omega\lambda|)}{\gamma|p||\omega_2|(1+\delta(a-1))}\right)^{\frac{1}{n-1}}\right\}$, where $\alpha, \beta, \gamma, \delta \in (0, 1)$ and $g(z) = az + b$ is a contraction mapping with $a, b \in \mathbb{C}$ and $|a| < 1$. Then $|z_k| \rightarrow \infty$, as $k \rightarrow \infty$, where $\{z_k\}$ is defined in (3.1).

Proof

From the construction of $U_\beta z_k$, we have

$$|U_\beta z_k| = |((1 - \beta)I + \beta U)(z_k)|, \quad k \geq 0.$$

For $k = 0$ and using (2.5), we have

$$\begin{aligned} |U_\beta z_0| &= |(1 - \beta)z_0 + \beta U(z_0)| \\ &= |(1 - \beta)z_0 + \beta(pe^{z_0^n} + qz_0 + r)| \\ &\geq |\beta(pe^{z_0^n} + qz_0 + r)| - (1 - \beta)|z_0| \\ &\geq \beta|p||e^{z_0^n}| - \beta|q||z_0| - \beta|r| - (1 - \beta)|z_0| \\ &\geq \beta|p||\omega_1||z_0^n| - \beta|q||z_0| - \beta|r| - (1 - \beta)|z_0|. \end{aligned}$$

Our assumption $|z_0| \geq \max\{|r|, |b|\}$ implies that $-|r| \geq -|z_0|$, therefore, we obtain

$$\begin{aligned} |U_\beta z_0| &\geq \beta|p||\omega_1||z_0^n| - \beta|q||z_0| - \beta|z_0| - (1 - \beta)|z_0| \\ &\geq \beta|p||\omega_1||z_0^n| - \beta|q||z_0| - |z_0|, \\ &= |z_0|(\beta|p||\omega_1||z_0^{n-1}| - (1 + \beta|q|)), \end{aligned}$$

thus,

$$|U_\beta z_0| \geq |z_0|(\beta|p||\omega_1||z_0^{n-1}| - (1 + \beta|q|)). \tag{3.2}$$

Using (3.1) and (3.2), we have

$$\begin{aligned} |y_0| &= |\alpha g(z_0) + (1 - \alpha)\mathcal{J}_\mu^{B_2} U_\beta z_0| \\ &= \left| \alpha(az_0 + b) + (1 - \alpha)\frac{U_\beta z_0}{1 + m\mu} \right| \\ &\geq (1 - \alpha)\frac{|U_\beta z_0|}{|1 + m\mu|} - \alpha|a||z_0| - \alpha|b| \\ &\geq (1 - \alpha)\frac{|z_0|(\beta|p||\omega_1||z_0|^{n-1} - (1 + \beta|q|))}{|1 + m\mu|} - \alpha|a||z_0| - \alpha|z_0| \\ &\geq |z_0|\left(\frac{(1 - \alpha)\beta|p||\omega_1||z_0|^{n-1} - (1 - \alpha)(1 + \beta|q|)}{|1 + m\mu|} - \alpha(1 + |a|)\right). \end{aligned}$$

Thus, we have

$$|y_0| \geq |z_0|\left(\frac{(1 - \alpha)\beta|p||\omega_1||z_0|^{n-1} - (1 - \alpha)(1 + \beta|q|)}{|1 + m\mu|} - \alpha(1 + |a|)\right). \tag{3.3}$$

Our assumption $|z_0| > \left(\frac{(1+\alpha(1+|a|))|1+m\mu|+(1-\alpha)(1+\beta|q|)}{(1-\alpha)\beta|p||\omega_1|}\right)^{\frac{1}{n-1}}$ gives

$$\frac{(1 - \alpha)\beta|p||\omega_1||z_0|^{n-1} - (1 - \alpha)(1 + \beta|q|)}{|1 + m\mu|} - \alpha(1 + |a|) > 1.$$

From (3.3), we obtain

$$|y_0| > |z_0|. \quad (3.4)$$

Now, from the construction of V_γ , we have

$$\begin{aligned} |V_\gamma y_0| &= |(1-\gamma)y_0 + \gamma V y_0| \\ &= |(1-\gamma)y_0 + \gamma(pe^{y_0^n} + qy_0 + r)| \\ &\geq |\gamma(pe^{y_0^n} + qy_0 + r)| - (1-\gamma)|y_0| \\ &\geq \gamma|p||e^{y_0^n}| - \gamma|q||y_0| - \gamma|r| - (1-\gamma)|y_0| \\ &\geq \gamma|p||\omega_2||y_0^n| - \gamma|q||y_0| - \gamma|r| - (1-\gamma)|y_0|. \end{aligned} \quad (3.5)$$

Using (3.4), (3.5) becomes

$$|V_\gamma y_0| \geq \gamma|p||\omega_2||z_0^n| - \gamma|q||z_0| - \gamma|r| - (1-\gamma)|z_0|. \quad (3.6)$$

The assumption $|z_0| \geq \max\{|r|, |b|\}$ implies that $-|r| \geq -|z_0|$, therefore, we obtain

$$\begin{aligned} |V_\gamma y_0| &\geq \gamma|p||\omega_2||z_0^n| - \gamma|q||z_0| - \gamma|z_0| - (1-\gamma)|z_0| \\ &\geq \gamma|p||\omega_2||z_0^n| - (1+\gamma|q|)|z_0|, \\ &= |z_0|(\gamma|p||\omega_2||z_0^{n-1}| - (1+\gamma|q|)). \end{aligned} \quad (3.7)$$

Now, from the construction of $S_\delta V_\gamma$, we have

$$\begin{aligned} S_\delta V_\gamma y_0 &= [(1-\delta)I + \delta S](V_\gamma y_0) \\ &= (1-\delta)V_\gamma y_0 + \delta S(V_\gamma y_0) \\ &= (1-\delta)V_\gamma y_0 + \delta(aV_\gamma y_0 + b) \\ &= (1+\delta(a-1))V_\gamma y_0 + \delta b. \end{aligned}$$

Therefore,

$$S_\delta V_\gamma y_0 = (1+\delta(a-1))V_\gamma y_0 + \delta b. \quad (3.8)$$

Further, from (3.1), consider

$$|z_1| = \left| \mathcal{J}_\lambda^{B_1} S_\delta V_\gamma y_0 \right|.$$

From (3.8), we have

$$\begin{aligned} |z_1| &= \left| \mathcal{J}_\lambda^{B_1} ((1+\delta(a-1))V_\gamma y_0 + \delta b) \right| \\ &= \left| \frac{((1+\delta(a-1))V_\gamma y_0 + \delta b)}{1+\omega\lambda} \right| \\ &\geq \left| \frac{(1+\delta(a-1))}{1+\omega\lambda} \right| |V_\gamma y_0| - \left| \frac{\delta b}{1+\omega\lambda} \right| \\ &\geq \frac{|(1+\delta(a-1))|}{|1+\omega\lambda|} |V_\gamma y_0| - \frac{\delta}{|1+\omega\lambda|} |b| \\ &\geq \frac{|(1+\delta(a-1))|}{|1+\omega\lambda|} |V_\gamma y_0| - \frac{\delta}{|1+\omega\lambda|} |z_0|. \end{aligned}$$

From (3.6), we have

$$|z_1| \geq |z_0| \left(\frac{|(1 + \delta(a - 1))|}{|1 + \omega\lambda|} (\gamma|p||\omega_2||z_0^{n-1}| - (1 + \gamma|q|)) - \frac{\delta}{|1 + \omega\lambda|} \right). \tag{3.9}$$

Our assumptions $|z_0| \geq \max\{|c|, |b|\} > \left(\frac{(1 + \gamma|q|)}{\gamma|p||\omega_2|} + \frac{(\delta + |1 + \omega\lambda|)}{\gamma|p||\omega_2|(1 + \delta(a - 1))} \right)^{\frac{1}{n-1}}$, gives

$$\frac{|(1 + \delta(a - 1))|}{|1 + \omega\lambda|} (\gamma|p||\omega_2||z_0^{n-1}| - (1 + \gamma|q|)) - \frac{\delta}{|1 + \omega\lambda|} > 1.$$

Thus, there exist a real number $\Omega > 0$ such that

$$\frac{|(1 + \delta(a - 1))|}{|1 + \omega\lambda|} (\gamma|p||\omega_2||z_0^{n-1}| - (1 + \gamma|q|)) - \frac{\delta}{|1 + \omega\lambda|} > \Omega + 1 > 1. \tag{3.10}$$

Using (3.9) and (3.10), we have

$$|z_1| > (1 + \Omega)|z_0|.$$

In particular $|z_1| > |z_0|$, on continuing the above procedure, we obtain $|z_k| > (1 + \Omega)^k|z_0|$. Hence, $|z_k| \rightarrow \infty$, as $k \rightarrow \infty$. \square

In the proof of Theorem 3.1, we have used only the fact that $|z_0| \geq \max\{|r|, |b|\} > \max \left\{ \left(\frac{(1+\alpha(1+|a|))|1+m\mu|+(1-\alpha)(1+\beta|q|)}{(1-\alpha)\beta|p||\omega_1|} \right)^{\frac{1}{n-1}}, \left(\frac{(1 + \gamma|q|)}{\gamma|p||\omega_2|} + \frac{(\delta + |1 + \omega\lambda|)}{\gamma|p||\omega_2|(1 + \delta(a - 1))} \right)^{\frac{1}{n-1}} \right\}$. So, we can refine it and obtain the following corollary.

Corollary 3.1

Let $|z_0| \geq \max \left\{ |r|, |b|, \left(\frac{(1+\alpha(1+|a|))|1+m\mu|+(1-\alpha)(1+\beta|q|)}{(1-\alpha)\beta|p||\omega_1|} \right)^{\frac{1}{n-1}}, \left(\frac{(1 + \gamma|q|)}{\gamma|p||\omega_2|} + \frac{(\delta + |1 + \omega\lambda|)}{\gamma|p||\omega_2|(1 + \delta(a - 1))} \right)^{\frac{1}{n-1}} \right\}$. Then $|z_k| \rightarrow \infty$, as $k \rightarrow \infty$.

Corollary 3.2

Let $|z_l| \geq \max \left\{ |r|, |b|, \left(\frac{(1+\alpha(1+|a|))|1+m\mu|+(1-\alpha)(1+\beta|q|)}{(1-\alpha)\beta|p||\omega_1|} \right)^{\frac{1}{n-1}}, \left(\frac{(1 + \gamma|q|)}{\gamma|p||\omega_2|} + \frac{(\delta + |1 + \omega\lambda|)}{\gamma|p||\omega_2|(1 + \delta(a - 1))} \right)^{\frac{1}{n-1}} \right\}$, for some $l \geq 0$. Then, there exists $\Omega > 0$ such that $|z_{l+k}| > (1 + \Omega)^k|z_l|$ and we have $|z_k| \rightarrow \infty$, as $k \rightarrow \infty$.

3.2. Escape criterion for $T(z) = \cos(z^n) + dz + c$

In this section, we prove the escape criteria for transcendental function $T(z) = \cos(z^n) + dz + c$, where $n \geq 2, d, c \in \mathbb{C}$ via generalized viscosity approximation-type iterative method. Also, let $U = V = T$ and $S = g$, where T is given in (2.3).

Theorem 3.2

Let $T(z) = \cos(z^n) + dz + c$ be a complex function, where $n \geq 2, d, c \in \mathbb{C}$. Assume that $z_0 \in \mathbb{C}, |z_0| \geq \max\{|c|, |b|\} > \max \left\{ \left(\frac{(1+\alpha(1+|a|))|1+m\mu|+(1-\alpha)(1+\beta|d|)}{(1-\alpha)\beta|\omega_1|} \right)^{\frac{1}{n-1}}, \left(\frac{(1 + \gamma|d|)}{\gamma|\omega_2|} + \frac{(\delta + |1 + \omega\lambda|)}{\gamma|\omega_2|(1 + \delta(a - 1))} \right)^{\frac{1}{n-1}} \right\}$, where $\alpha, \beta, \gamma, \delta \in (0, 1)$. Then $|z_k| \rightarrow \infty$, as $k \rightarrow \infty$, where $\{z_k\}$ is defined in (3.1).

Proof

From the construction of $U_\beta z_k$, we have

$$|U_\beta z_k| = |((1 - \beta)I + \beta U)(z_k)|, \quad k \geq 0.$$

For $k = 0$ and using (2.5), we have

$$\begin{aligned} |U_\beta z_0| &= |(1 - \beta)z_0 + \beta U(z_0)| \\ &= |(1 - \beta)z_0 + \beta(\cos(z^n) + dz + c)| \\ &\geq |\beta(\cos(z^n) + dz + c)| - (1 - \beta)|z_0| \\ &\geq \beta|\cos(z^n)| - \beta|d||z_0| - \beta|c| - (1 - \beta)|z_0| \\ &\geq \beta|\omega_2||z_0^n| - \beta|d||z_0| - \beta|c| - (1 - \beta)|z_0|. \end{aligned}$$

Our assumption $|z_0| \geq \max\{|c|, |b|\}$ implies that $-|c| \geq -|z_0|$, therefore, we obtain

$$\begin{aligned} |U_\beta z_0| &\geq \beta|\omega_2||z_0^n| - \beta|d||z_0| - \beta|z_0| - (1 - \beta)|z_0| \\ &\geq \beta|\omega_2||z_0^n| - \beta|d||z_0| - |z_0|, \\ &= |z_0|(\beta|\omega_2||z_0^{n-1}| - (1 + \beta|d|)), \end{aligned}$$

thus,

$$|U_\beta z_0| \geq |z_0|(\beta|\omega_2||z_0^{n-1}| - (1 + \beta|d|)). \quad (3.11)$$

Using (3.1) and (3.11), we have

$$\begin{aligned} |y_0| &= |\alpha g(z_0) + (1 - \alpha)\mathcal{J}_\mu^{B_2} U_\beta z_0| \\ &= \left| \alpha(az_0 + b) + (1 - \alpha)\frac{U_\beta z_0}{1 + m\mu} \right| \\ &\geq (1 - \alpha)\frac{|U_\beta z_0|}{|1 + m\mu|} - \alpha|a||z_0| - \alpha|b| \\ &\geq (1 - \alpha)\frac{|z_0|(\beta|\omega_2||z_0^{n-1}| - (1 + \beta|d|))}{|1 + m\mu|} - \alpha|a||z_0| - \alpha|z_0| \\ &\geq |z_0| \left(\frac{(1 - \alpha)\beta|\omega_2||z_0^{n-1}| - (1 - \alpha)(1 + \beta|d|)}{|1 + m\mu|} - \alpha(1 + |a|) \right). \end{aligned}$$

Thus, we have

$$|y_0| \geq |z_0| \left(\frac{(1 - \alpha)\beta|\omega_2||z_0^{n-1}| - (1 - \alpha)(1 + \beta|d|)}{|1 + m\mu|} - \alpha(1 + |a|) \right). \quad (3.12)$$

Our assumption $|z_0| > \left(\frac{(1 + \alpha(1 + |a|))|1 + m\mu| + (1 - \alpha)(1 + \beta|d|)}{(1 - \alpha)\beta|\omega_2|} \right)^{\frac{1}{n-1}}$ gives

$$\frac{(1 - \alpha)\beta|\omega_2||z_0^{n-1}| - (1 - \alpha)(1 + \beta|d|)}{|1 + m\mu|} - \alpha(1 + |a|) > 1.$$

From (3.12), we obtain

$$|y_0| > |z_0|. \quad (3.13)$$

Now, from the construction of V_γ , we have

$$\begin{aligned} |V_\gamma y_0| &= |(1 - \gamma)y_0 + \gamma V y_0| \\ &= |(1 - \gamma)y_0 + \gamma(\cos(y_0^n) + dy_0 + c)| \\ &\geq |\gamma(\cos(y_0^n) + dy_0 + c)| - (1 - \gamma)|y_0| \\ &\geq \gamma|\cos(y_0^n)| - \gamma|d||y_0| - \gamma|c| - (1 - \gamma)|y_0| \\ &\geq \gamma|\omega_2||y_0^n| - \gamma|d||y_0| - \gamma|c| - (1 - \gamma)|y_0|. \end{aligned} \quad (3.14)$$

Using (3.13), (3.14) becomes

$$|V_\gamma y_0| \geq \gamma|\omega_2||z_0^n| - \gamma|d||z_0| - \gamma|c| - (1 - \gamma)|z_0|. \tag{3.15}$$

The assumption $|z_0| \geq \max\{|c|, |b|\}$ implies that $-|c| \geq -|z_0|$, therefore, we obtain

$$\begin{aligned} |V_\gamma y_0| &\geq \gamma|\omega_2||z_0^n| - \gamma|d||z_0| - \gamma|z_0| - (1 - \gamma)|z_0| \\ &\geq \gamma|\omega_2||z_0^n| - (1 + \gamma|d|)|z_0|, \\ &= |z_0|(\gamma|\omega_2||z_0^{n-1}| - (1 + \gamma|d|)). \end{aligned} \tag{3.16}$$

Now, from the construction of $S_\delta V_\gamma$, we have

$$\begin{aligned} S_\delta V_\gamma y_0 &= [(1 - \delta)I + \delta S](V_\gamma y_0) \\ &= (1 - \delta)V_\gamma y_0 + \delta(aV_\gamma y_0 + b) \\ &= (1 + \delta(a - 1))V_\gamma y_0 + \delta b. \end{aligned}$$

Therefore,

$$S_\delta V_\gamma y_0 = (1 + \delta(a - 1))V_\gamma y_0 + \delta b. \tag{3.17}$$

Further, from (3.1), consider

$$|z_1| = \left| \mathcal{J}_\lambda^{B_1} S_\delta V_\gamma y_0 \right|.$$

From (3.17), we have

$$\begin{aligned} |z_1| &= \left| \mathcal{J}_\lambda^{B_1} ((1 + \delta(a - 1))V_\gamma y_0 + \delta b) \right| \\ &= \left| \frac{((1 + \delta(a - 1))V_\gamma y_0 + \delta b)}{1 + \omega\lambda} \right| \\ &\geq \frac{|(1 + \delta(a - 1))|}{|1 + \omega\lambda|} |V_\gamma y_0| - \frac{\delta}{|1 + \omega\lambda|} |b| \\ &\geq \frac{|(1 + \delta(a - 1))|}{|1 + \omega\lambda|} |V_\gamma y_0| - \frac{\delta}{|1 + \omega\lambda|} |z_0|. \end{aligned}$$

From (3.15), we have

$$|z_1| \geq |z_0| \left(\frac{|(1 + \delta(a - 1))|}{|1 + \omega\lambda|} (\gamma|\omega_2||z_0^{n-1}| - (1 + \gamma|d|)) - \frac{\delta}{|1 + \omega\lambda|} \right). \tag{3.18}$$

Our assumptions $|z_0| \geq \max\{|c|, |b|\} > \left(\frac{(1 + \gamma|d|)}{\gamma|\omega_2|} + \frac{(\delta + |1 + \omega\lambda|)}{\gamma|\omega_2||1 + \delta(a - 1)|} \right)^{\frac{1}{n-1}}$, gives

$$\frac{|(1 + \delta(a - 1))|}{|1 + \omega\lambda|} (\gamma|\omega_2||z_0^{n-1}| - (1 + \gamma|d|)) - \frac{\delta}{|1 + \omega\lambda|} > 1.$$

Thus, there exist a real number $\Omega > 0$ such that

$$\frac{|(1 + \delta(a - 1))|}{|1 + \omega\lambda|} (\gamma|\omega_2||z_0^{n-1}| - (1 + \gamma|d|)) - \frac{\delta}{|1 + \omega\lambda|} > \eta + 1 > 1. \tag{3.19}$$

Using (3.18) and (3.19), we have

$$|z_1| > (1 + \eta)|z_0|.$$

In particular $|z_1| > |z_0|$, on continuing the above procedure, we obtain $|z_k| > (1 + \eta)^k |z_0|$. Hence, $|z_k| \rightarrow \infty$, as $k \rightarrow \infty$. □

In the proof of Theorem 3.2, we have used only the fact that $|z_0| \geq \max\{|c|, |b|\} > \max\left\{\left(\frac{(1+\alpha(1+|a|))|1+m\mu|+(1-\alpha)(1+\beta|d|)}{(1-\alpha)\beta|\omega_2|}\right)^{\frac{1}{n-1}}, \left(\frac{(1+\gamma|d|)}{\gamma|\omega_2|} + \frac{(\delta+|1+\omega\lambda|)}{\gamma|\omega_2||1+\delta(a-1)|}\right)^{\frac{1}{n-1}}\right\}$. So, we can refine it and obtain the following corollary.

Corollary 3.3

Let $|z_0| \geq \max\left\{|c|, |b|, \left(\frac{(1+\alpha(1+|a|))|1+m\mu|+(1-\alpha)(1+\beta|d|)}{(1-\alpha)\beta|\omega_2|}\right)^{\frac{1}{n-1}}, \left(\frac{(1+\gamma|d|)}{\gamma|\omega_2|} + \frac{(\delta+|1+\omega\lambda|)}{\gamma|\omega_2||1+\delta(a-1)|}\right)^{\frac{1}{n-1}}\right\}$.
Then $|z_k| \rightarrow \infty$, as $k \rightarrow \infty$.

4. Generation of Julia sets

We attempt to obtain the non-classical Julia sets in four distinct orbits using Matlab R2019a (9.6.0.1072779) 64-bit. To visualize the fractals, we tailor two algorithms: one for the Julia set of $W(z) = pe^{z^n} + qz + r$ and the other for $T(z) = \cos(z^n) + dz + c$ employing the generalized viscosity approximation-type iterative method, where $n \geq 2$ and $p, q, r, d, c \in \mathbb{C}$. We sketch some graphs of Julia sets at different input parameters and different values of n , generating Julia sets through the generalized viscosity approximation-type iterative method using Algorithms 1 and 2. Throughout the paper, a maximum number of iterations $K = 70$ is consistently applied.

Algorithm 1 Geometry of Viscosity Julia set for $W(z) = pe^{z^n} + qz + r$

Input: $W(z) = pe^{z^n} + qz + r$, where $n \geq 2, p, q, r \in \mathbb{C}$, be a parameters for W ; K -maximal number of ; iterations A -area; $\alpha, \beta, \gamma, \delta \in (0, 1)$ -parameters of the generalized viscosity approximation-type iterative method; $g(z) = az + b$, where $a, b \in \mathbb{C}$ and $|a| < 1$; colourmap[0.. C -1]-color with C colors.

Output: Julia set for area A

for $z_0 \in A$ **do**

$$R = \max\left\{|r|, |b|, \left(\frac{(1+\alpha(1+|a|))|1+m\mu|+(1-\alpha)(1+\beta|q|)}{(1-\alpha)\beta|p|\omega_1|}\right)^{\frac{1}{n-1}}, \left(\frac{(1+\gamma|q|)}{\gamma|p|\omega_2|} + \frac{(\delta+|1+\omega\lambda|)}{\gamma|p|\omega_2||1+\delta(a-1)|}\right)^{\frac{1}{n-1}}\right\}.$$

$$k = 0$$

while $k \leq K$ **do**

$$z_{k+1} = \frac{(1+\delta(a-1))[(1-\gamma)y_k + \gamma W(y_k)] + \delta b}{(1+\omega\lambda)}$$

$$y_k = \alpha g(z) + (1-\alpha) \frac{\nu}{(1+m\mu)}$$

$$\nu = (1-\beta)z + \beta W(z)$$

if $|z_{k+1}| \geq R$ **then**

break

end if

$$k = k + 1$$

end while

$$i = \lfloor (C-1) \frac{k}{K} \rfloor$$

colour z_0 with colourmap [i]

Algorithm 2 Geometry of Viscosity Julia set for $T(z) = \cos(z^n) + dz + c$

Input: $T(z) = \cos(z^n) + dz + c$, where $n \geq 2, c, d \in \mathbb{C}$, be a parameters for T ; K -maximal number of ; iterations A -area; $\alpha, \beta, \gamma, \delta \in (0, 1)$ -parameters of the generalized viscosity approximation-type iterative method; $g(z) = az + b$, where $a, b \in \mathbb{C}$ and $|a| < 1$; colourmap[0.. C -1]-color with C colors.

Output: Julia set for area A

```

for  $z_0 \in A$  do

$$R = \max \left\{ |c|, |b|, \left( \frac{(1+\alpha(1+|a|))|1+m\mu|+(1-\alpha)(1+\beta|d|)}{(1-\alpha)\beta|\omega_2|} \right)^{\frac{1}{n-1}}, \left( \frac{(1+\gamma|d|)}{\gamma|\omega_2|} + \frac{(\delta+|1+\omega\lambda|)}{\gamma|\omega_2||1+\delta(a-1)|} \right)^{\frac{1}{n-1}} \right\}.$$

 $k = 0$ 
while  $k \leq K$  do

$$z_{k+1} = \frac{(1+\delta(a-1))[(1-\gamma)y_k+\gamma T(y_k)]+\delta b}{(1+\omega\lambda)}$$


$$y_k = \alpha g(z) + (1-\alpha) \frac{\nu}{(1+m\mu)}$$


$$\nu = (1-\beta)z + \beta T(z)$$

if  $|z_{k+1}| \geq R$  then
    break
end if
 $k = k + 1$ 
end while
 $i = \lfloor (C-1) \frac{k}{K} \rfloor$ 
colour  $z_0$  with colourmap [ $i$ ]

```



Figure 1. Colour map used in the generation of viscosity Julia sets examples

4.1. Julia sets for $W(z) = pe^{z^n} + qz + r$

In the first example, we generate Julia sets via Algorithm 1 for $W(z) = pe^{z^n} + qz + r$, where $n \geq 2$ and $p, q, r \in \mathbb{C}$. The parameters used to generate the sets in this example were the following: $n = 2, p = 5 + 4i, q = 9.1 + 13.1i, r = 3 + 12i, a = 0.25 + 0.36i, b = -0.001 - 0.001i, m = 0.004, \omega = 0.0013, \mu = 0.1, \lambda = 0.3, |w_1| = 0.81, |w_2| = 0.75$. In the example, we divided the images into four groups. In each group, we fix three parameters from $\alpha, \beta, \gamma, \delta$ and vary the remaining one.

- In Figure 2, we see images generated for fixed $\beta = 0.25, \gamma = 0.45, \delta = 0.65$, and varying α : (a) 0.15, (b) 0.45, (c) 0.85.
- In Figure 3, we see images generated for fixed $\alpha = 0.01, \gamma = 0.002, \delta = 0.007$, and varying β : (a) 0.15, (b) 0.45, (c) 0.85.
- In Figure 4, we see images generated for fixed $\alpha = 0.1, \beta = 0.35, \delta = 0.55$, and varying γ : (a) 0.15, (b) 0.45, (c) 0.85.
- In Figure 5, we see images generated for fixed $\alpha = 0.02, \beta = 0.04, \gamma = 0.06$, and varying δ : (a) 0.15, (b) 0.45, (c) 0.85.

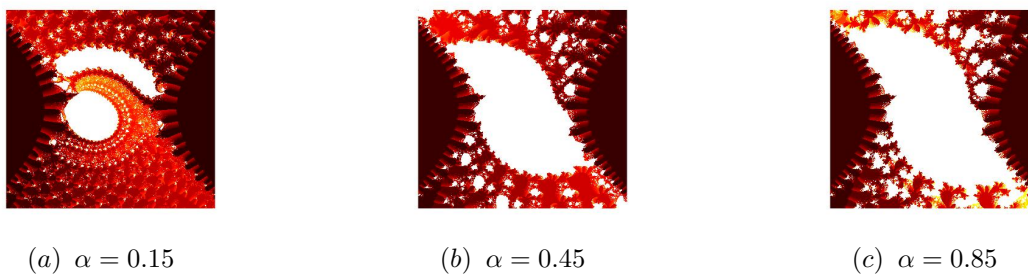


Figure 2. Julia sets for $n = 2$ with $\beta = 0.25, \gamma = 0.45, \delta = 0.65$ and varying α

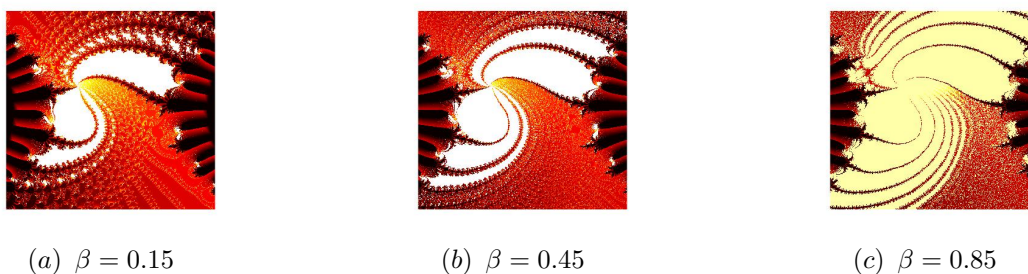


Figure 3. Julia sets for $n = 2$ with $\alpha = 0.01, \gamma = 0.002, \delta = 0.007$ and varying β

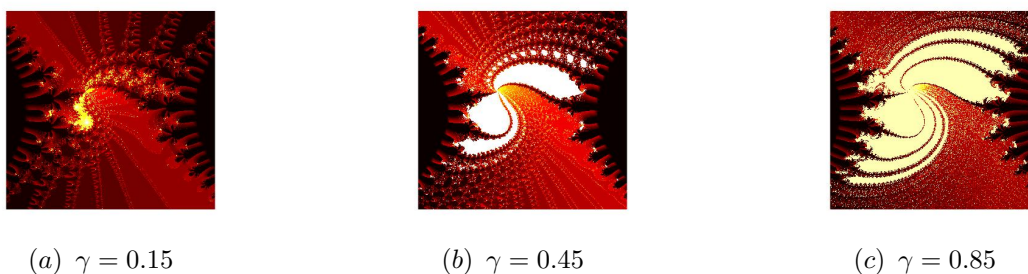


Figure 4. Julia sets for $n = 2$ with $\alpha = 0.1, \beta = 0.35, \delta = 0.55$ and varying γ

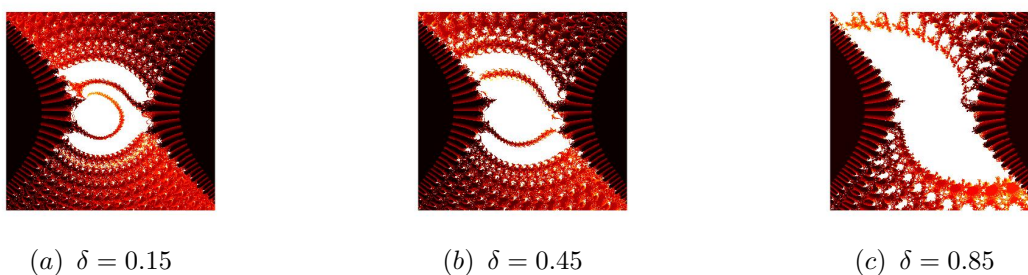


Figure 5. Julia sets for $n = 2$ with $\alpha = 0.02, \beta = 0.04, \gamma = 0.06$ and varying δ

In Figures 2-5 (a, b, c), for $n = 2$, we fixed the value of three parameters from $\alpha, \beta, \gamma, \delta$ and varied the remaining one. From the images, we see that the α, β, γ and δ parameters have a great impact on the shape, size and color of the set. For low values of varying parameters, the amount of red colour in the Julia set decreases from the center. Moreover, we can observe that for lower values of the varying parameter, the shape change is smaller than for higher values of the varying parameter, and the generated Julia sets look like flowers and Rangoli, or may be compared to glass paintings.

In the second example, the parameters used to generate the sets in this example were the following: $n = 4, p = 91 + 201i, q = 91 + 13i, r = 3 + 12i, a = 0.25 + 0.36i, b = 0.0001 + 0.0003i, m = .004, \omega = 0.3, \mu = 0.4, \lambda = 0.3, |w_1| = 0.55, |w_2| = 0.35$. In this example, we divided the images into four groups. In each group, we fix three parameters from $\alpha, \beta, \gamma, \delta$ and vary the remaining one.

- In Fig. 6, we see images generated for fixed $\beta = 0.035, \gamma = 0.045, \delta = 0.065$, and varying α : (a) 0.015, (b) 0.045, (c) 0.085.
- In Fig. 7, we see images generated for fixed $\alpha = 0.41, \gamma = 0.61, \delta = 0.81$, and varying β : (a) 0.015, (b) 0.045, (c) 0.085.
- In Fig. 8, we see images generated for fixed $\alpha = 0.1, \beta = 0.5, \delta = 0.8$, and varying γ : (a) 0.0015, (b) 0.0045, (c) 0.0085.
- In Fig. 9, we see images generated for fixed $\alpha = 0.002, \beta = 0.007, \gamma = 0.006$, and varying δ : (a) 0.35, (b) 0.65, (c) 0.85.

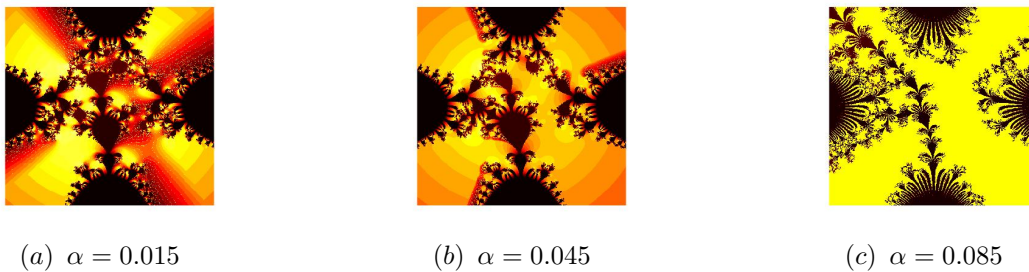


Figure 6. Julia sets for $n = 4$ with $\beta = 0.035, \gamma = 0.045, \delta = 0.065$ and varying α

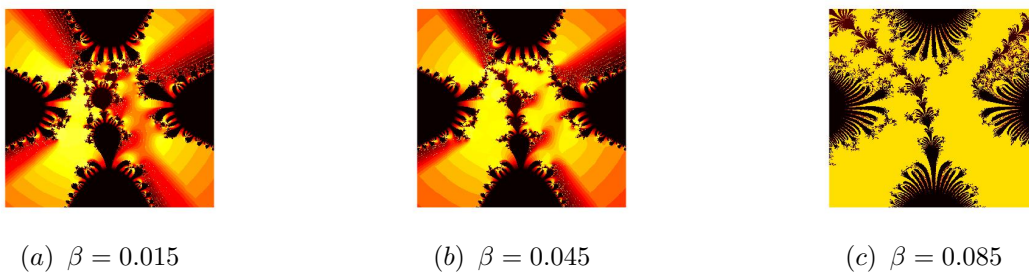


Figure 7. Julia sets for $n = 4$ with $\alpha = 0.41, \gamma = 0.61, \delta = 0.81$ and varying β

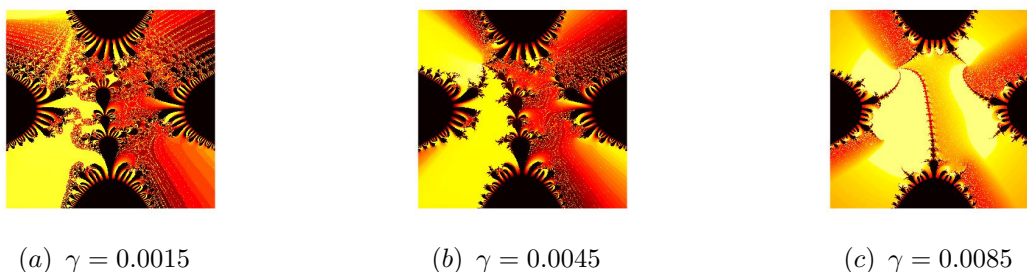


Figure 8. Julia sets for $n = 4$ with $\alpha = 0.1, \beta = 0.5, \delta = 0.8$ and varying γ

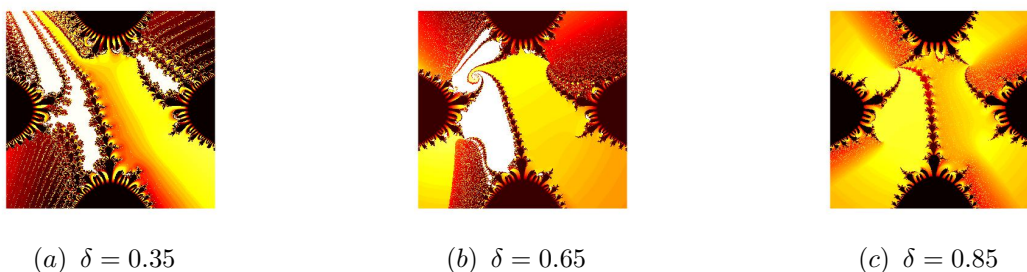


Figure 9. Julia sets for $n = 4$ with $\alpha = 0.002, \beta = 0.007, \gamma = 0.006$, and varying δ

In Figures 6-9 (a, b, c), for $n = 4$, we fixed the value of three parameters from $\alpha, \beta, \gamma, \delta$ and varied the remaining one. As the different values of the parameters α, β, γ and δ increase, we can observe that the shape change is that the bulb size is smaller than in cases with higher values of the varying parameters, and the generated Julia sets look like flowers and Rangoli, or may be compared to glass painting.

In the third example, the parameters used to generate the sets in this example were the following: $n = 2, m = 0.4, \omega = 0.13, \mu = 0.5, \lambda = 0.1, |w_1| = 0.85, |w_2| = 0.45, \alpha = 0.01, \beta = 0.03, \gamma = 0.08, \delta = 0.05$. In this example, we divided the images into four groups. In each group, we fix three parameters from p, q, r, b and vary the remaining one.

- In Fig. 10, we see images generated for fixed $q = 15.5, r = 4.5, b = 2.5$, and varying p : (a) 1.5, (b) $1.5i$, (c) $0.01 + 0.03i$.
- In Fig. 11, we see images generated for fixed $p = 5.75, r = 4.5, b = 2.5$, and varying q : (a) 14.5, (b) $14.5i$, (c) $8 + 14.5i$.
- In Fig. 12, we see images generated for fixed $p = 2.25, q = 7.8, b = 2.5$, and varying r : (a) 17.5, (b) $17.5i$, (c) $0.1 + 0.01i$.
- In Fig. 13, we see images generated for fixed $p = 0.3i, q = 18.1, r = 5.5i$, and varying b : (a) 24, (b) $2.5i$, (c) $8.5 + 0.17i$.

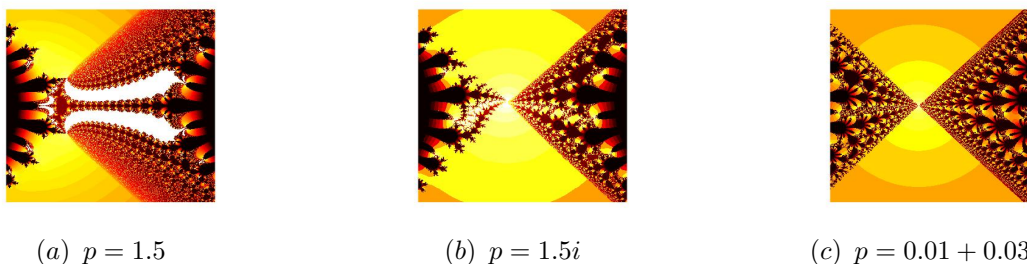


Figure 10. Julia sets for $n = 2$ with fixed $q = 15.5, r = 4.5, b = 2.5$ and varying p

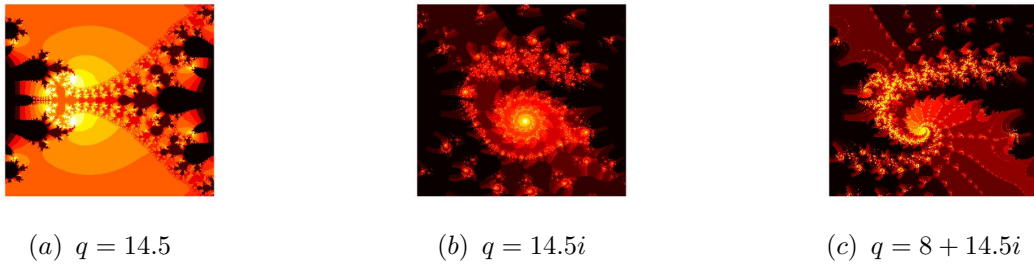


Figure 11. Julia sets for $n = 2$ with fixed $p = 5.75, r = 4.5, b = 2.5$ and varying q

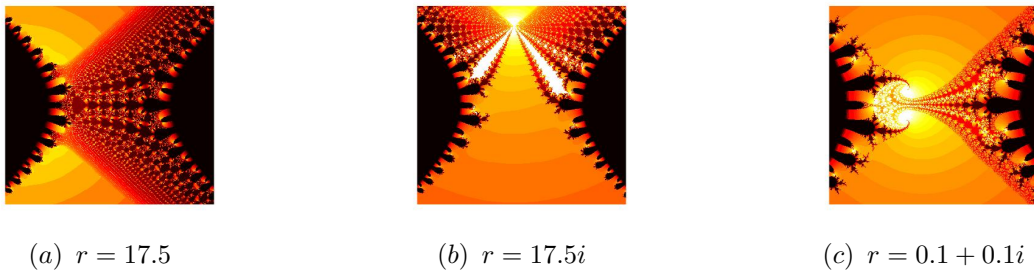


Figure 12. Julia sets for $n = 2$ with fixed $p = 2.25, q = 7.8, b = 2.5$ and varying r

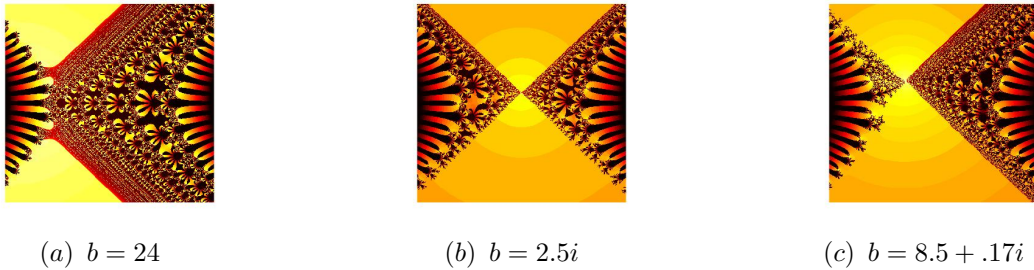


Figure 13. Julia sets for $n = 2$ with fixed $p = 0.3i, q = 18.1, r = 5.5i$ and varying b

In fourth example, we show the variety of Julia sets that can be generated by generalized viscosity approximation-type iterative method for $W(z) = pe^{z^2} + qz + r$, where $n \geq 2$ and $p, q, r \in \mathbb{C}$. They are presented in Fig.14 (a)-(f), and the parameters used to generate them were the following:

- (a) $W(z) = 0.13e^{z^2} + 17.5z + 12.1, g(z) = 0.8z + 11.1, m = 0.02, \omega = 0.03, \mu = 0.81, \lambda = 0.2,$
 $|w_1| = 0.81, |w_2| = 0.75, \alpha = 0.08, \beta = 0.06, \gamma = 0.04, \delta = 0.075,$
- (b) $W(z) = -0.13e^{z^2} - 17.5z - 12.1, g(z) = -0.8z - 11.1, m = 0.02, \omega = 0.03, \mu = 0.81, \lambda = 0.2,$
 $|w_1| = 0.81, |w_2| = 0.75, \alpha = 0.08, \beta = 0.06, \gamma = 0.04, \delta = 0.075,$
- (c) $W(z) = 0.013ie^{z^2} + 0.17iz + 5.2i, g(z) = 0.8iz + 3.1i, m = -1.02, \omega = -1.4, \mu = 0.3, \lambda = 0.2,$
 $|w_1| = 0.81, |w_2| = 0.75, \alpha = 0.08, \beta = 0.06, \gamma = 0.04, \delta = 0.075,$
- (d) $W(z) = -0.013ie^{z^2} - 0.17iz - 5.2i, g(z) = -0.8iz - 3.1i, m = -1.02, \omega = -1.4, \mu = 0.3,$
 $\lambda = 0.2, |w_1| = 0.81, |w_2| = 0.75, \alpha = 0.08, \beta = 0.06, \gamma = 0.04, \delta = 0.075,$
- (e) $W(z) = (0.003 + 0.008i)e^{z^2} + (0.02 + 0.03i)z + 3 + 5i, g(z) = (0.025 + 0.005i)z + 0.003 + 0.004i,$
 $m = -0.42, \omega = -1.014, \mu = 0.41, \lambda = 0.32, |w_1| = 0.81, |w_2| = 0.75, \alpha = 0.08, \beta = 0.06, \gamma = 0.04,$
 $\delta = 0.075,$
- (f) $W(z) = (-0.003 - 0.008i)e^{z^2} + (-0.02 - 0.03i)z - 3 - 5i, g(z) = (-0.025 - 0.005i)z - 0.003 -$
 $0.004i, m = -0.42, \omega = -1.014, \mu = 0.41, \lambda = 0.32, |w_1| = 0.81, |w_2| = 0.75, \alpha = 0.08, \beta = 0.06,$
 $\gamma = 0.04, \delta = 0.075,$

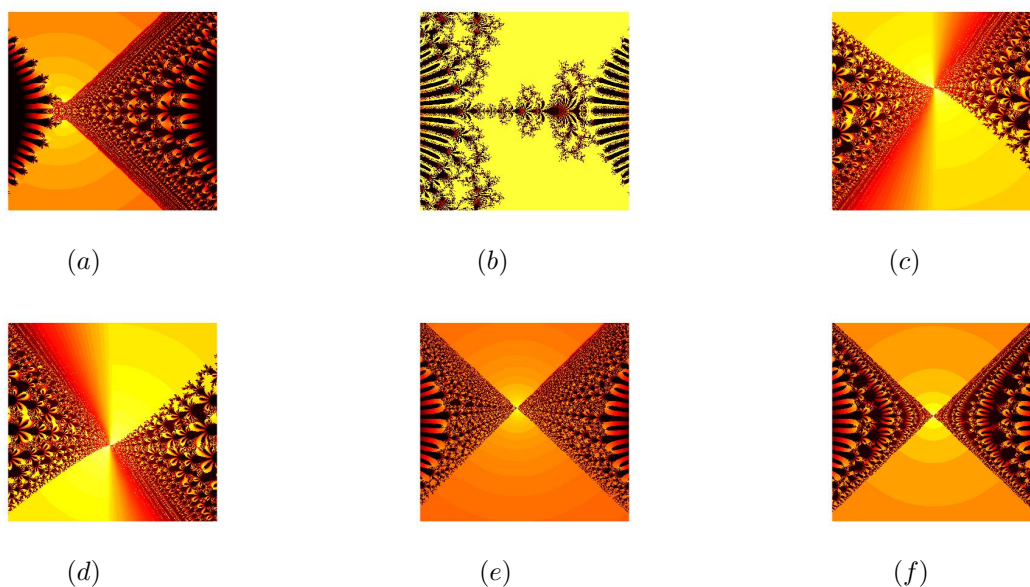


Figure 14. Julia sets for $n = 2$ via generalized viscosity approximation-type iterative method

As the different values of the parameters p, q and r , we notice that when the values of the parameters p, q and r are positive as well as negative real numbers, we clearly see that the value of the parameters has a major impact on the shape of the Julia set and its size (see, Figure 14 (a, b)). Also, we notice that for the complex values of p, q and r , we observe that, for a given value of 'n', we obtain looking like 'n' copies of the pyramid-shaped Julia sets, which are joined end to end, and we see an opposite tendency (see, Figure 14 (c)-(f)). Moreover, we can observe that the set has a 2-fold symmetry.

In this example, we show the variety of Julia sets that can be generated by generalized viscosity approximation-type iterative method for $W(z) = pe^{z^n} + qz + r$, where $n \geq 2$ and $p, q, r \in \mathbb{C}$. They are presented in Fig.15 (a)-(f), and the parameters used to generate them were the following:

- (a) $n = 2, W(z) = -6.75e^{z^2} - 17.5iz + 2.5i, g(z) = 0.8z + 1.5, m = 0.02, \omega = 0.03, \mu = 0.01, \lambda = 0.05, |w_1| = 0.81, |w_2| = 0.75, \alpha = 0.001, \beta = 0.05, \gamma = 0.002, \delta = 0.003,$
- (b) $n = 4, W(z) = (41.9 - 5.3i)e^{z^4} + (-2.5 - 7.9i)z - 2.2i, g(z) = 0.8iz + 11i, m = 0.02, \omega = 0.04, \mu = 0.03, \lambda = 0.05, |w_1| = 0.81, |w_2| = 0.75, \alpha = 0.08, \beta = 0.06, \gamma = 0.04, \delta = 0.075,$
- (c) $n = 5, W(z) = (33 - 7.3i)e^{z^5} - (2.5 + 7.9i)z - 2.5i, g(z) = -0.8iz + 11.5, m = 0.02, \omega = 0.04, \mu = 0.03, \lambda = 0.05, |w_1| = 0.81, |w_2| = 0.75, \alpha = 0.08, \beta = 0.06, \gamma = 0.04, \delta = 0.075,$
- (d) $n = 17, W(z) = (-9 - 3.3i)e^{z^{17}} + 17.5iz + 2.5i, g(z) = 0.75z + 16.5i, m = 0.02, \omega = 0.04, \mu = 0.03, \lambda = 0.05, |w_1| = 0.81, |w_2| = 0.75, \alpha = 0.08, \beta = 0.06, \gamma = 0.04, \delta = 0.075,$
- (e) $n = 22, W(z) = (-9 - 3.3i)e^{z^{22}} + 17.5iz + 2.5i, g(z) = 0.75z + 16.5i, m = 0.02, \omega = 0.04, \mu = 0.03, \lambda = 0.05, |w_1| = 0.81, |w_2| = 0.75, \alpha = 0.08, \beta = 0.06, \gamma = 0.04, \delta = 0.075,$
- (f) $n = 35, W(z) = (-9 - 3.3i)e^{z^{35}} + 17.5iz + 2.5i, g(z) = 0.75z + 16.5i, m = 0.02, \omega = 0.04, \mu = 0.03, \lambda = 0.05, |w_1| = 0.81, |w_2| = 0.75, \alpha = 0.08, \beta = 0.06, \gamma = 0.04, \delta = 0.075.$

As the different value of n , we notice that when the value of n increases, we clearly see that the value of n has a great impact on the shape of the Julia set and its size. Moreover, we see that the generated Julia set becomes more complex with the increase in the value of n (see, Figure 15 (a)-(f)).

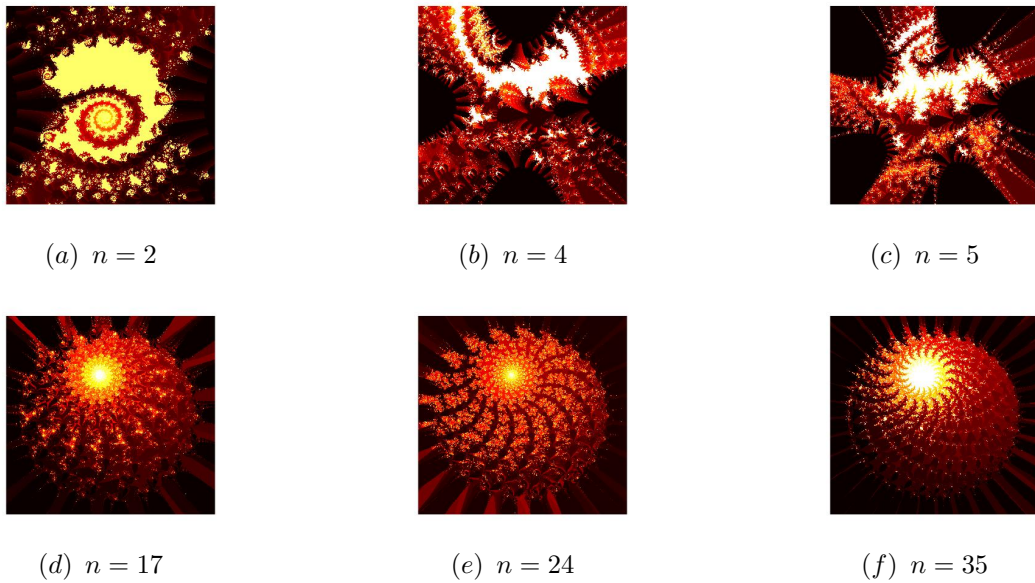


Figure 15. Julia sets for $n = 2$ via viscosity approximation-type iterative method with s -convexity with $\gamma = 9$ and varying t .

4.2. Julia sets for $T(z) = \cos(z^n) + dz + c$

In next example, we generate Julia sets Algorithm 2 for $T(z) = \cos(z^n) + dz + c$, where $n \geq 2$ and $d, c \in \mathbb{C}$. The parameters used to generate the sets in this example were the following: $n = 2, d = 10.5, c = 7.5, a = 0.75, b = 5.5, m = 0.1, \omega = 0.3, \mu = 0.4, \lambda = 0.5, |w_1| = 0.25, |w_2| = 0.45$. In this example, we divided the images into four groups. In each group, we fix three parameters from $\alpha, \beta, \gamma, \delta$ and vary the remaining one.

- In Fig. 16, we see images generated for fixed $\beta = 0.012, \gamma = 0.025, \delta = 0.045$, and varying α : (a) 0.0125, (b) 0.225, (c) 0.725.
- In Fig. 17, we see images generated for fixed $\alpha = 0.01, \gamma = 0.025, \delta = 0.047$, and varying β : (a) 0.0125, (b) 0.425, (c) 0.625.
- In Fig. 18, we see images generated for fixed $\alpha = 0.1, \beta = 0.25, \delta = 0.45$, and varying γ : (a) 0.0125, (b) 0.225, (c) 0.425.
- In Fig. 19, we see images generated for fixed $\alpha = 0.5, \beta = 0.6, \gamma = 0.7$, and varying δ : (a) 0.00001, (b) 0.0002, (c) 0.003.

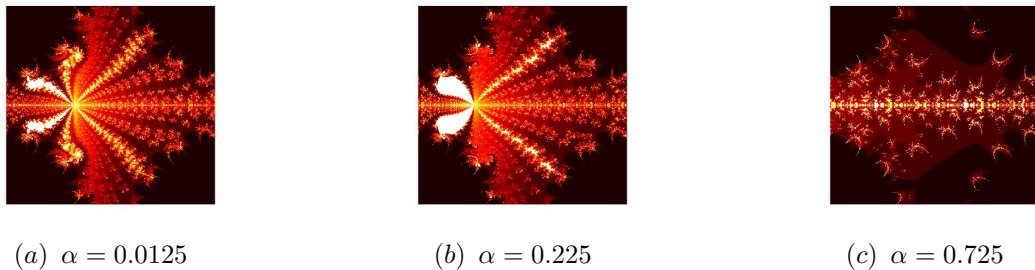


Figure 16. Julia sets for $n = 2$ with fixed $\beta = 0.012, \gamma = 0.025, \delta = 0.045$, and varying α

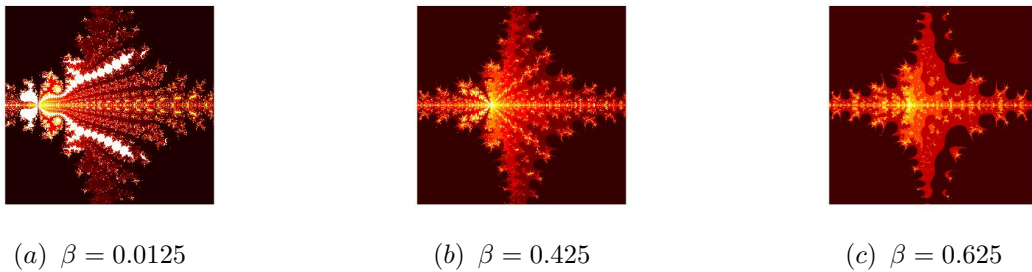


Figure 17. Julia sets for $n = 2$ with fixed $\alpha = 0.01, \gamma = 0.025, \delta = 0.047$, and varying β

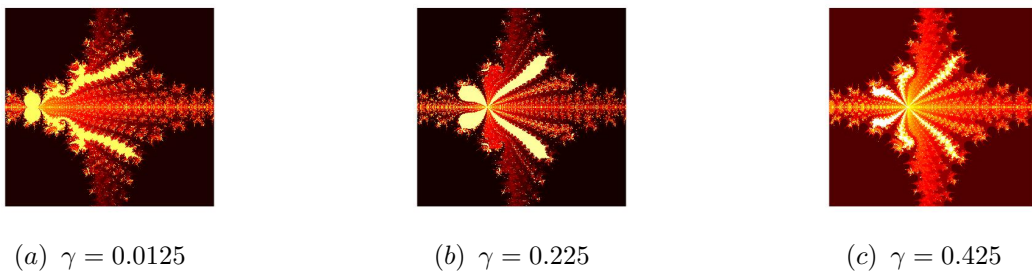


Figure 18. Julia sets for $n = 2$ with fixed $\alpha = 0.1, \beta = 0.25, \delta = 0.45$, and varying γ

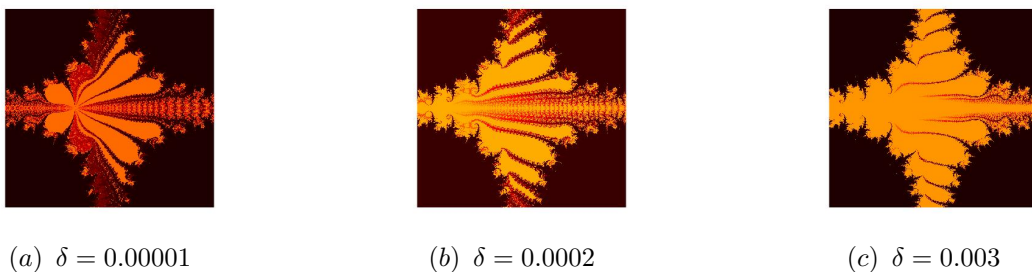


Figure 19. Julia sets for $n = 2$ with fixed $\alpha = 0.5, \beta = 0.6, \gamma = 0.7$, and varying δ

In Figures 16-19, we fixed the value of three parameters from $\alpha, \beta, \gamma, \delta$ and varied the remaining one. From the images, we see that the α, β, γ and δ parameters have a great impact on the shape, size, and colour of the set. In Figures 16-19 (a, b) and 17-19 (c), we obtain the fractals are looking like ants, and in Figures 16-17(c), we also notice that when the value of the varying parameter increases, then the set loses its connectivity and tends to a dust-like set. In the next example, we generate Julia sets by Algorithm 2 for $T(z) = \cos(z^n) + dz + c$, where $n \geq 2$ and $d, c \in \mathbb{C}$. The parameters used to generate the sets in this example were the following: $n = 2, m = 0.01, \omega = 0.02, \mu = 0.03, \lambda = 0.04, |w_1| = 0.45, |w_2| = 0.65, \alpha = 0.001, \beta = 0.02, \gamma = 0.003, \delta = 0.02$. In this example, we divided the images into four groups. In each group, we fix three parameters from c, d, b and vary the remaining one.

- In Fig. 20, we see images generated for fixed $c = 4.5, b = 2.5$, and varying d : (a) 11.5, (b) 13.5i, (c) $11 + 13.5i$.
- In Fig. 21, we see images generated for fixed $d = 13.1i, b = 2.5$, and varying c : (a) 6.5, (b) 11.5i, (c) $2.5 - 19i$.
- In Fig. 22, we see images generated for fixed $d = 11.9 + 14.4i, c = 6.5$, and varying b : (a) 19.5, (b) 4.25i, (c) $5.5 - 1.17i$.

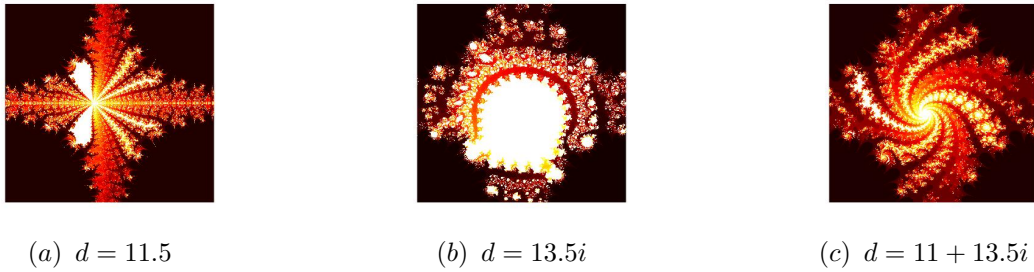


Figure 20. Julia sets for $n = 2$ with fixed $c = 4.5, b = 2.5$, and varying d

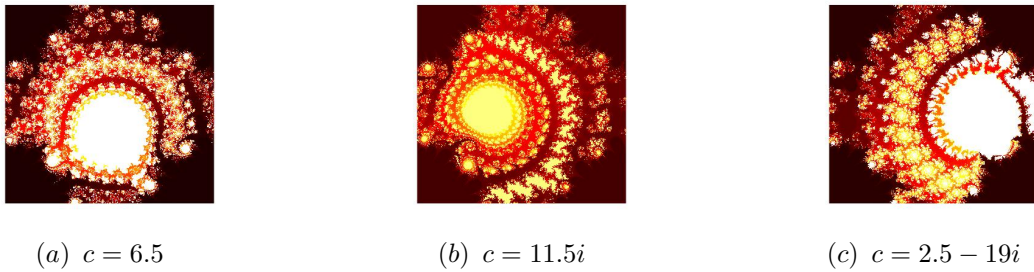


Figure 21. Julia sets for $n = 2$ with fixed $d = 13.1i, b = 2.5$, and varying c

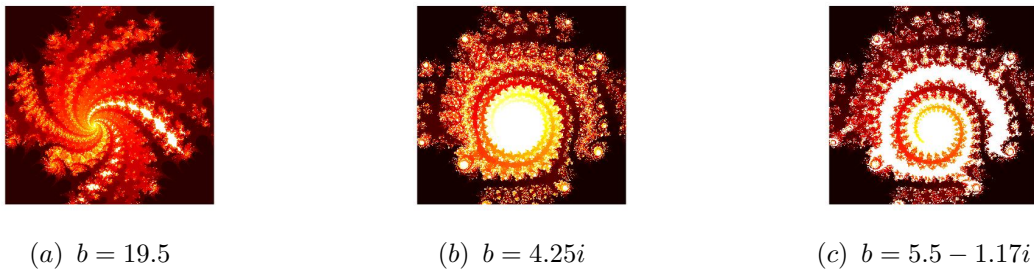


Figure 22. Julia sets for $n = 2$ with fixed $d = 11.9 + 14.4i, c = 6.5$, and varying b

In Figures 20-22, we fixed the value of two parameters from d, c, b and varied the remaining one. We notice that when the value of a varying parameter changes from real to complex, we clearly see that the imaginary parts of d, c and b plays an important role in obtaining the swirls in the pattern, colourful teething ring or circular saw or may be compared to glass painting. Moreover, the fractals are looking like ants, see Figure 20(a). In this example, we show the variety of Julia sets that can be generated by generalized viscosity approximation-type iterative method for $T(z) = \cos(z^n) + dz + c$, where $n \geq 2$ and $d, c \in \mathbb{C}$. They are presented in Fig. 23 (a)-(f), and the parameters used to generate them were the following:

- (a) $n = 3, W(z) = \cos(z^3) + 15.5iz + 0.75i, g(z) = 0.85iz + 1.05i, m = 0.004, \omega = 0.01, \mu = 0.02,$
 $\lambda = 0.03, |w_1| = 0.85, |w_2| = 0.75, \alpha = 0.003, \beta = 0.02, \gamma = 0.002, \delta = 0.003,$
- (b) $n = 5, W(z) = \cos(z^4) + 15.5iz + 0.75i, g(z) = 0.85iz + 1.05i, m = 0.004, \omega = 0.01, \mu = 0.02,$
 $\lambda = 0.03, |w_1| = 0.85, |w_2| = 0.75, \alpha = 0.003, \beta = 0.02, \gamma = 0.002, \delta = 0.003,$
- (c) $n = 7, W(z) = \cos(z^5) + 11.5iz + 0.75i, g(z) = 0.15iz + 2.05i, m = 0.004, \omega = 0.01, \mu = 0.02,$
 $\lambda = 0.03, |w_1| = 0.85, |w_2| = 0.75, \alpha = 0.003, \beta = 0.02, \gamma = 0.002, \delta = 0.003,$
- (d) $n = 13, W(z) = \cos(z^{13}) + 15.5iz + 2.5i, g(z) = 0.01iz + 1.5i, m = 0.004, \omega = 0.01, \mu = 0.02,$
 $\lambda = 0.03, |w_1| = 0.85, |w_2| = 0.75, \alpha = 0.003, \beta = 0.02, \gamma = 0.002, \delta = 0.003,$
- (e) $n = 21, W(z) = \cos(z^{22}) + 11.5iz + 2.5i, g(z) = 0.85z + 1.5i, m = 0.004, \omega = 0.01, \mu = 0.02,$
 $\lambda = 0.03, |w_1| = 0.85, |w_2| = 0.75, \alpha = 0.003, \beta = 0.02, \gamma = 0.002, \delta = 0.003,$

(f) $n = 37$, $W(z) = \cos(z^{37}) + 12.5iz + 2.5$, $g(z) = 0.85z + 11.5i$, $m = 0.004$, $\omega = 0.01$, $\mu = 0.02$,
 $\lambda = 0.03$, $|w_1| = 0.85$, $|w_2| = 0.75$, $\alpha = 0.003$, $\beta = 0.02$, $\gamma = 0.002$, $\delta = 0.003$,

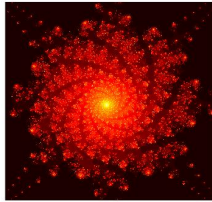
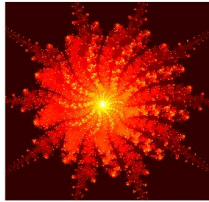
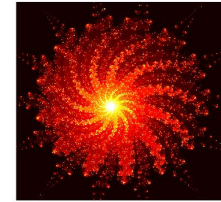
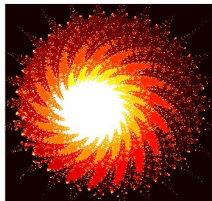
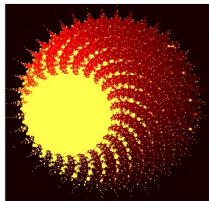
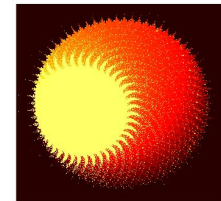
(a) $n = 3$ (b) $n = 5$ (c) $n = 7$ (d) $n = 13$ (e) $n = 21$ (f) $n = 37$

Figure 23. Julia sets via generalized viscosity approximation-type iterative method and varying n .

As the different value of n , we notice that when the value of n increases, we clearly see that the value of n has a great impact on the shape of the Julia set and its size. Moreover, we see that the generated Julia set becomes more complex and the main body shape changes with the increase in the value of n (see, Figures 23 (a)-(f)). In Figure 2-23, all the figures look-like ants, swirls in the pattern, colourful teething rings or circular saws or may be compared to glass paintings but have differences in Julia points. For the different values of the parameters, and more beauty is added to the swirl pattern. It is seen that

- the parameters p, q, r, d, c and b play a very important role in giving shape, size, and colour to the fractals.
- the convergence criteria derived for the fractals are also playing a very crucial role in determining the resolution and richness of the pixels in the fractals.
- all the fractals developed in this paper are very novel, aesthetic, and pleasing as the complex functions $W(z)$ and $T(z)$.

5. Conclusion

We derived an escape criterion for generating fractals using the proposed iterative method for the complex functions $W(z) = pe^{z^n} + qz + r$ and $T(z) = \cos(z^n) + dz + c$ where $n \geq 2$ and $p, q, r, d, c \in \mathbb{C}$. The visualization of Julia sets is facilitated by implementing these results in Algorithms 1 and 2. Using MATLAB software, we produced interesting non-classical variants of the Julia fractals, which we can discuss and evaluate for various parameter values. We expect that these results will be helpful in the study of the various fractal varieties that were initially mentioned. We believe that the results of this research will be valuable for those interested in creating aesthetically pleasing graphics and designer printing patterns. Additionally, the textile sector can benefit from these findings for designing and printing purposes.

Acknowledgement

The authors would like to express their gratitude to the anonymous referees and editor for their valuable suggestions and helpful comments which led to significant improvement of the original manuscript of this paper.

REFERENCES

1. I. Ahmad, M. Sajid and R. Ahmad, *Julia sets of transcendental functions via a viscosity approximation-type iterative method with s -convexity*, Stat., Optim. Inf. Comput., vol. 12, pp. 0–19, 2024.
2. P. Blanchard, R. Devaney, A. Garijo and E. Russell, *A generalized version of the McMullen domain*, Int. J. Bifurcation Chaos, vol. 18, no. 8, pp. 2309–2318, 2008.
3. S. Costanzo and F. Venneri, *Polarization-insensitive fractal metamaterial surface for energy harvesting in IoT applications*, Electronics, vol. 9, no. 6, pp. 959, 2020.
4. B. Halpern, *Fixed points of non-expanding maps*, Bull. Am. Math. Soc., vol. 73, pp. 957–961, 1967.
5. L. Jolaoso and S. Khan, *Some escape time results for general complex polynomials and biomorphs generation by a new iteration process*, Mathematics, vol. 8, no. 12, pp. 2172, 2020.
6. L. Jolaoso, S. Khan and K. Aremu, *Dynamics of RK iteration and basic family of iterations for polynomiography*, Mathematics, vol. 10, no. 18, pp. 3324, 2022.
7. G. Julia, *Memoire sur l'iteration des fonctions rationnelles*, Pures Appl., vol. 8, pp. 47–245, 1918.
8. S. M. Kang, A. Rafiq, A. Latif, A. A. Shahid, and Y. C. Kwun, *Tricorns and Multicorns of S -iteration scheme*, J. Funct. Spaces, vol. 2015, Article ID 417167, pp. 197–203.
9. S. Kumari, K. Gdawiec, A. Nandal, M. Postolache and R. Chugh, *A novel approach to generate Mandelbrot sets, Julia sets and biomorphs via viscosity approximation method*, Chaos Solitons Fractals, vol. 163, pp. 112–140, 2022.
10. W.J. Krzysztofik, *Fractals in antennas and metamaterials applications*. In: F. Brambila (ed) *Fractal Analysis-Applications in Physics*, Engineering and Technology, IntechOpen, vol. 2017, pp. 953–978, 2017.
11. Y. C. Kwun, M. Tanveer, W. Nazeer, M. Abas, and S. M. Kang, *Fractal Generation in Modified Jungck- S Orbit*, IEEE Access, vol. 235, pp. 35060–35071, 2019.
12. A. Lakhtakia, V. Varadan, R. Messier and V. Varadan, *On the symmetries of the Julia sets for the process $z \rightarrow z^p + c$* , J. Phys. A: Math. Gen., vol. 20, no. 11, pp. 3533–3535, 1987.
13. B. Mandelbrot, *The Fractal Geometry of Nature*, W.H. Freeman and Company, New York, 1983.
14. A. Maudafi, *Viscosity approximation methods for fixed-points problems*, J. Math. Anal. Appl., vol. 241, no. 1, pp. 46–55, 2000.
15. W.R. Mann, *Mean value methods in iteration*, Proc. Am. Math. Soc., vol. 4, no. 3, pp. 506–510, 1953.
16. P. Muthukumar and P. Balasubramaniam, *Feedback synchronization of the fractional order reverse butterfly-shaped chaotic system and its application to digital cryptography*, Nonlinear Dyn., vol. 74, pp. 1169–1181, 2013.
17. A. Nandal, R. Chugh and M. Postolache, *Iteration process for fixed point problems and zero of maximal monotone operators*, Symmetry, vol. 11, no. 5, pp. 655, 2019.
18. K. Nakamura, *Iterated inversion system: An algorithm for efficiently visualizing Kleinian groups and extending the possibilities of fractal art*, J. Math. Arts, vol. 15, no. 9, pp. 106–136, 2021.
19. P. C. Ouyang, K. W. Chung, A. Nicolas and K. Gdawiec, *Self-similar fractal drawings inspired by M. C. Escher's print square limit*, ACM Trans. Graphic., vol. 40, pp. 1–34, 2021.
20. W. Phuengrattana and S. Suantai, *On the rate of convergence of Mann, Ishikawa, Noor and SP -iterations for continuous functions on an arbitrary interval*, J. Comput. Appl. Math., vol. 235, no. 9, pp. 3006–3014, 2011.
21. B. Prasad and K. Katiyar, *Fractals via Ishikawa iteration*, Commun. Comp. Inf. Sci., vol. 140, pp. 197–203, 2011.
22. M. Rani and R. Agarwa, *Effect of stochastic noise on superior Julia sets*, J. Math. Im. Vis., vol. 36, no. 1, pp. 63–77, 2010.
23. M. Rani and V. Kumar, *Superior Julia sets*, J. Korea Soc. Math. Educ. Ser. D Res. Math. Educ., vol. 2004, no. 8, pp. 261–277, 2004.
24. A. A. Shahid, W. Nazeer and K. Gdawiec, *The Picard-Mann iteration with s -convexity in the generation of Mandelbrot and Julia sets*, Monatsh. Math., vol. 195, pp. 565–584, 2021.
25. S. Kumari, K. Gdawiec, A. Nandal, N. Kumar and R. Chugh, *On the viscosity approximation type iterative method and its non-linear behavior in the generation of Mandelbrot and Julia sets*, Numer. Algorithms, vol. 2023, 2023.
26. S. Kumari, K. Gdawiec, A. Nandal, N. Kumar and R. Chugh, *An Application of Viscosity Approximation Type Iterative Method in the Generation of Mandelbrot and Julia Fractals*, Aequat. Math., vol. 97, pp. 257–278, 2023.
27. M. Tanveer, W. Nazeer and K. Gdawiec, *New escape criteria for complex fractals generation in Jungck- CR orbit*, Indian J. Pure Appl. Math., vol. 51, pp. 1285–1303, 2020.
28. A. Tomar, V. Kumar, U.S. Rana and M. Sajid, *Fractals as Julia and Mandelbrot sets of complex cosine function via fixed point iterations*, Symmetry, vol. 7, no. 6, pp. 10939–10957, 2022.
29. G. I. Usurelu, A. Bejenaru and M. Postolache, *Newton-like methods and polynomiographic visualization of modified Thakur processes*, Int. J. Comput. Math., vol. 98, pp. 1049–1068, 2021.
30. X. Zhang, L. Wang, Z. Zhou and Y. Niu, *A chaos-based image encryption technique utilizing Hilbert curves and H -fractals*, IEEE Access, vol. 7, pp. 74734–74746, 2019.